

# SALCA-IB: Self-Adaptive LLM-Driven Continuous Learning Agent for IB Network Failure Prediction

**Abstract**—The proliferation of transformer-based large language models has intensified demands on high-performance computing infrastructure, where InfiniBand (IB) networks are crucial for their superior low-latency and high-bandwidth communication capabilities. Network failures in these environments can trigger significant training interruptions or necessitate complete restarts, leading to substantial computational resource waste and training cost overhead. However, effective failure prediction faces dual challenges: the scarcity of failure data and the vulnerability of network features to environmental variations. This paper introduces SALCA-IB (Self-Adaptive LLM-Driven Continuous Learning Agent for IB Network Failure Prediction), an innovative system that leverages Large Language Models (LLMs) as its planning core. The system’s key innovations comprise: (1) LLM-driven autonomous data selection and model optimization; (2) A dual-memory fusion system integrating short-term and long-term memory mechanisms; and (3) LLM-supported automatic evaluation feedback with closed-loop optimization. Experimental results on a production cluster with 2,048 computing cards demonstrate that SALCA-IB enhances prediction F1@K-score by 5.1% in static scenarios and achieves a 19.1% improvement when confronting network feature distribution shifts, substantially advancing the predictability of large-scale computing infrastructure.

**Index Terms**—InfiniBand Network, Large Language Model, Autonomous Agent

## I. INTRODUCTION

The unprecedented evolution of transformer-based language models has revolutionized the artificial intelligence landscape, imposing extraordinary demands on computing infrastructure. Training these increasingly sophisticated models, which frequently encompass hundreds of billions of parameters, necessitates extensive distributed computing resources equipped with high-performance interconnects. Within this computational ecosystem, InfiniBand (IB) networks have emerged as the de facto standard, distinguished by their superior low-latency and high-bandwidth communication capabilities, thereby forming the essential backbone for distributed training operations.

Network failures in distributed training environments can have severe consequences. When IB network failures occur during model training, they often trigger unexpected training interruptions or necessitate complete restarts, leading to significant computational resource waste and increased operational costs. For instance, recent studies have shown that network-related failures can account for up to 30% of training interruptions in large-scale AI clusters, with each incident potentially wasting hundreds of GPU hours (He et al. [6]). This challenge becomes particularly acute as models grow larger and training runs extend to weeks or even months.

Despite its paramount importance, effective IB network failure prediction confronts multiple fundamental challenges. Primarily, failure data in production environments exhibits inherent scarcity, as failure events remain relatively rare in well-maintained systems, thereby impeding the development of robust prediction models through conventional machine learning approaches. Furthermore, network feature distributions demonstrate high dynamicity and vulnerability to diverse external factors (Liu et al. [8]), including environmental conditions, hardware degradation, and maintenance interventions. These challenges are intensified by the escalating scale and architectural complexity of modern computing infrastructures.

Traditional approaches to network failure prediction predominantly rely on static machine learning models or rule-based systems (Mohammed et al. [9], Nie et al. [10]). Although these methods demonstrate efficacy in controlled environments, they exhibit significant performance degradation in real-world scenarios where network characteristics undergo continuous evolution. Furthermore, existing solutions typically function as black boxes, offering limited interpretability while failing to effectively utilize historical experience for systematic improvement (Das et al. [5]). While recent advances in deep learning-based approaches have endeavored to address these limitations, they continue to encounter substantial challenges in adapting to dynamic environments and maintaining sustained prediction accuracy (Alharthi et al. [2]).

The advent of Large Language Models (LLMs) introduces promising avenues for addressing these challenges. LLMs have exhibited exceptional capabilities in complex reasoning and strategic planning tasks (Ahmed et al. [1], Su et al. [12]), indicating their potential as orchestrators for adaptive prediction systems. Moreover, recent innovations in memory systems and continuous learning architectures (Zhang et al. [13]) demonstrate significant promise in managing dynamic environments, although their application to IB network failure prediction remains substantially underexplored.

To address these challenges, we propose SALCA-IB (Self-Adaptive LLM-Driven Continuous Learning Agent for IB Network Failure Prediction), an innovative system that combines the reasoning capabilities of LLMs with traditional machine learning models in a unified, adaptive framework. To tackle the data scarcity challenge, SALCA-IB employs an LLM-driven planning core that intelligently orchestrates data selection and model optimization. To handle dynamic feature distributions, we design a dual-memory system that integrates both short-term and long-term experiences. Furthermore, to ensure sustained prediction accuracy, we implement a continuous

learning mechanism with LLM-supported feedback loops that enables real-time adaptation to changing network conditions.

The main contributions of this paper are threefold:

- We introduce a novel LLM-driven agent architecture for IB network failure prediction that strategically positions LLM as a high-level planning core to orchestrate model selection, parameter optimization, and continuous learning strategies, while deploying traditional machine learning models as efficient executors for real-time prediction tasks.
- We develop an innovative dual-memory fusion system that organically integrates short-term and long-term memory mechanisms, facilitating rapid adaptation to dynamic network variations while systematically preserving and leveraging historical knowledge to enhance prediction robustness.
- We perform extensive empirical evaluation on a large-scale production cluster comprising 2,048 computing cards, demonstrating that SALCA-IB achieves a 5.1% improvement in prediction F1@K-score under static conditions and realizes a 19.1% performance gain when confronting network feature distribution shifts. Through systematic ablation studies, we quantitatively validate the significant contributions of both the LLM-driven framework and the dual-memory system components.

The manuscript is structured as follows: Section II examines related work in HPC failure prediction and LLM agent applications. Section III elaborates on the architectural design and implementation details of SALCA-IB. Section IV presents comprehensive experimental methodology and results. Finally, Section V summarizes our findings and outlines future research directions.

## II. RELATED WORK

### A. HPC Clusters Failure Prediction

Failure prediction in HPC clusters, particularly for large-scale GPU training workloads, has garnered substantial research attention due to its fundamental role in maintaining system reliability. Conventional methodologies predominantly employ statistical analysis and machine learning techniques. He et al. [6] conducted comprehensive analyses of hardware failures in deep learning training systems, establishing that GPU failures substantially impact training progression and model convergence. In parallel, Liu et al. [8] specifically investigated GPU failure prediction under intensive deep learning workloads, illuminating the distinctive challenges inherent in monitoring and predicting failures within GPU-intensive computing environments.

Contemporary research has endeavored to address these challenges through ensemble methodologies and advanced deep learning approaches. Nie et al. [10] pioneered GPU error prediction models leveraging temporal and spatial dependencies to enhance prediction robustness under data-constrained conditions, conceptually aligned with our model pool architecture albeit lacking intelligent orchestration capabilities.

Das et al. [5] investigated LSTM-based architectures for system health prediction and failure lead time estimation, sharing conceptual similarities with our long-term memory mechanism but without incorporating continuous adaptation mechanisms. Liu et al. [8] further advanced the field through high-precision GPU failure prediction methods under deep learning workloads, demonstrating enhanced accuracy while still encountering limitations in dynamic environments. Despite these advancements, as emphasized by Alharthi et al. [2], existing methodologies continue to face substantial challenges in managing dynamic network environments and maintaining sustained prediction accuracy.

### B. LLM-based Reasoning and Self-Improvement

Recent advancements in LLM capabilities have revealed their significant potential in complex reasoning and self-improvement tasks. This evolution can be examined through two distinct perspectives:

1) *Reasoning and Verification*: LLMs have exhibited exceptional capabilities in complex reasoning tasks, albeit with specific constraints that warrant careful consideration. Chen et al. [18] established chain-of-thought prompting as a fundamental methodology for enhancing reasoning capabilities, while Wang et al. [19] extended this paradigm through a self-consistency framework that systematically evaluates multiple reasoning pathways. An et al. [24] subsequently demonstrated LLMs' capacity to enhance reasoning capabilities through error-driven learning, particularly when provided with structured feedback mechanisms. However, Tyen et al. [16] identified a critical limitation: while LLMs excel at guided correction, they exhibit significant limitations in autonomous error detection.

Contemporary research has focused on addressing these inherent limitations through diverse methodological approaches. Weng et al. [15] developed sophisticated self-verification mechanisms that substantially enhance reasoning reliability. Complementarily, Gou et al. [26] introduced CRITIC, an innovative framework enabling LLMs to perform self-correction through tool-interactive critiquing. These advancements in self-improvement capabilities hold particular significance for complex system monitoring and failure prediction tasks, where precise reasoning about system states is paramount.

2) *Continuous Learning and Adaptation*: The evolution of continuous learning capabilities in LLMs has demonstrated remarkable progress, particularly regarding their capacity for temporal adaptation and improvement. Madaan et al. [14] pioneered a self-improving framework wherein LLMs autonomously generate and evaluate optimization strategies. This foundational work was further enhanced by Gao et al. [25], who developed a comprehensive lifelong learning approach facilitating autonomous experiential learning in LLMs.

Several innovative frameworks have emerged to augment LLMs' adaptive capabilities. Qiao et al. [27] demonstrated enhanced tool learning through systematic execution feedback, while Shinn et al. [28] introduced Reflexion, a sophisticated framework for implementing verbal reinforcement learning

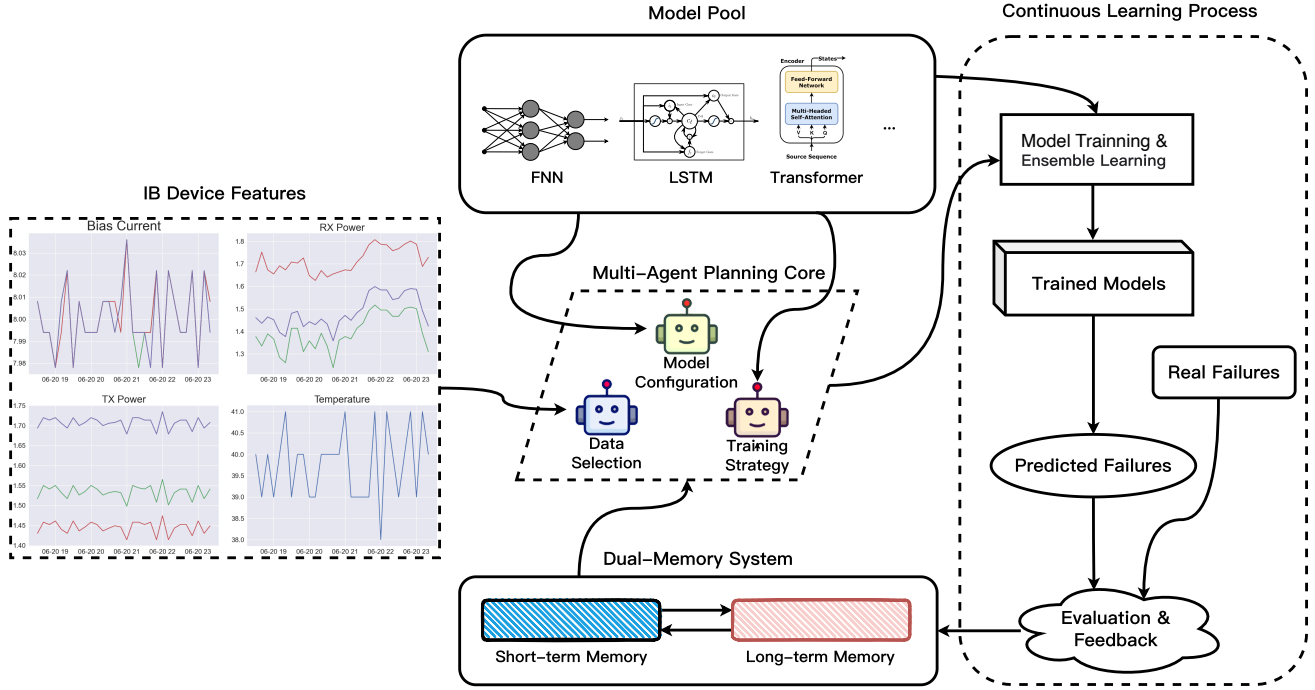


Fig. 1. Overview of SALCA-IB architecture. The system integrates (a) a model pool containing diverse deep learning models, (b) a multi-agent planning core for intelligent orchestration, (c) a dual-memory system for knowledge retention, and (d) a continuous learning process for adaptive optimization.

in language agents. These advances in continuous learning and adaptation mechanisms prove particularly pertinent for maintaining prediction accuracy in dynamic operational environments.

### C. LLM Applications in Time Series and Agent Systems

The integration of LLMs into time series analysis and agent-based systems represents an emerging research frontier, with particular relevance to failure prediction tasks.

1) *Time Series Analysis and Forecasting*: Recent investigations have demonstrated LLMs' efficacy in time series analysis tasks. Gruver et al. [34] established the feasibility of zero-shot time series forecasting using LLMs, while Jin et al. [35] developed Time-LLM, illustrating the potential for reprogramming LLMs specifically for time series forecasting applications. Cao et al. [32] introduced TEMPO, a sophisticated prompt-based framework engineered for precise time series prediction.

Contemporary methodological advances have focused on enhancing LLMs' temporal data processing capabilities. Chang et al. [33] developed novel techniques for optimizing pre-trained LLMs as data-efficient time series forecasters, while Zhou et al. [37] established a unified paradigm for comprehensive time series analysis utilizing pretrained language models. Xue et al. [36] introduced PromptCast, pioneering an innovative prompt-based learning framework specifically engineered for time series forecasting tasks.

2) *Multi-Agent and Workflow Systems*: The incorporation of LLMs into multi-agent and workflow systems has emerged as a promising paradigm for complex task orchestration. Wang

et al. [29] demonstrated that mixture-of-agents architectures substantially enhance LLM capabilities, particularly in managing complex, multi-step operational sequences. Wang et al. [30] pioneered agent workflow memory systems, addressing fundamental challenges in maintaining state consistency across extended operations.

These architectural advances have demonstrated particular efficacy in domain-specific applications. Yao et al. [31] established the viability of LLM-based approaches for multi-agent reasoning and action coordination, illustrating their potential for orchestrating complex, multi-entity prediction tasks. While these developments represent significant progress in both LLM capabilities and their practical applications, their potential for network failure prediction remains substantially under-explored, particularly regarding the challenges of dynamic network environments and real-time adaptation requirements.

## III. METHODOLOGY

SALCA-IB is designed as a self-adaptive intelligent system that leverages large language models (LLMs) to orchestrate network failure prediction in industrial blockchain environments. As illustrated in Fig. 2, the system integrates four key components: an LLM-driven planning core, a dual-memory system, a deep learning model pool, and a continuous learning process.

As shown in Algorithm 1, the LLM planning core serves as the system's central intelligence, orchestrating model selection, data processing, and strategy optimization. The dual-memory system combines short-term memory for rapid re-

sponse and long-term memory for knowledge retention, enabling both immediate adaptation and sustained optimization. The model pool comprises diverse deep learning models (MLP, LSTM, and Transformer) that serve as the execution layer for failure prediction. Through continuous learning, the system evaluates prediction outcomes and adjusts strategies dynamically, ensuring robust performance in evolving network conditions. The detailed design of each component is elaborated in the following sections.

#### A. LLM-Driven Planning Core

Traditional failure prediction systems often rely on static model architectures and fixed training strategies, limiting their effectiveness in dynamic IB environments. Our LLM-driven planning core addresses this challenge by orchestrating three key components: data selection, model configuration, and training strategy optimization, as shown in Fig. 2.

1) *Data Selection*: The data selection module processes IB network data streams  $\mathcal{D} = \{(X_t, y_t)\}_{t=1}^T$ , where  $X_t \in \mathbb{R}^{w \times d}$  represents a sequence of network states within a sliding window. Specifically,  $X_t = [x_{t-w+1}, \dots, x_t]$  where  $x_i \in \mathbb{R}^d$  contains  $d$  network features at time step  $i$ ,  $w$  is the window size (e.g., 30 time steps), and  $y_t \in \{0, 1\}$  indicates whether a failure occurs following this sequence. Given historical knowledge  $\mathcal{K} \subset \text{Mem}_{long}$ , the LLM performs reasoning-based selection through:

$$\mathcal{D}_{train} = f_{LLM}(\mathcal{D}, \mathcal{K}) = \{(X_i, y_i) | s_i > \tau, (X_i, y_i) \in \mathcal{D}\} \quad (1)$$

where  $s_i$  is the sequence importance score determined by LLM reasoning:

$$s_i = LLM(X_i, \mathcal{K}, \text{prompt}_{select}) \quad (2)$$

The LLM generates importance scores through a structured reasoning process that evaluates both temporal evolution patterns and feature interactions within each sequence. This evaluation process is guided by carefully designed prompts that encode domain knowledge about network failure progression patterns and their manifestation across multiple features over time.

The data selection process consists of three sequential components:

a) *Temporal Window Selection*: The LLM analyzes temporal context to determine optimal window configuration:

$$W_t^* = LLM(\{X_{t-k}, \dots, X_t\}, \mathcal{K}, \text{prompt}_{temporal}) \quad (3)$$

where  $\text{prompt}_{temporal}$  guides the analysis of multi-scale temporal dependencies. The window selection considers both the granularity of individual time steps and the overall sequence length needed to capture failure progression patterns.

b) *Distribution Assessment*: For selected windows, the LLM evaluates sequence representativeness:

$$q_i = LLM(X_i, W_t^*, \mathcal{K}, \text{prompt}_{distribution}) \quad (4)$$

This assessment examines both the temporal evolution of individual features and their cross-feature correlations within each

sequence. The evaluation particularly focuses on identifying characteristic patterns that historically preceded failure events.

c) *Final Selection*: The LLM integrates previous analyses for final sequence selection:

$$\mathcal{D}_{train} = \{(X_i, y_i) | LLM(q_i, \mathcal{K}, \text{prompt}_{final}) > \tau\} \quad (5)$$

The final selection phase considers the completeness and quality of feature sequences, ensuring selected samples contain meaningful progression patterns for failure prediction.

The prompt design for each component incorporates specific aspects of temporal sequence analysis and feature interaction patterns. This enables the LLM to identify and select sequences that best capture the progression of network states leading to potential failures, while considering both historical patterns and current network conditions.

2) *Model Configuration*: The model configuration module dynamically selects and configures prediction models based on both current data characteristics and historical performance patterns. Given a model pool  $\mathcal{M} = \{M_1, \dots, M_m\}$  containing various neural architectures (e.g., CNN, LSTM, Transformer), the LLM performs configuration through:

$$(M_{selected}, \Theta, S) = f_{LLM}^{config}(\mathcal{M}, \mathcal{K}, X_t) \quad (6)$$

where  $M_{selected} \subset \mathcal{M}$  is the selected model subset,  $\Theta$  represents their corresponding parameter configurations, and  $S$  defines the ensemble strategy. The configuration process consists of three key components:

a) *Architecture Selection*: The LLM evaluates and selects appropriate model architectures based on current sequence characteristics:

$$M_{selected} = LLM(\mathcal{M}, X_t, \mathcal{K}, \text{prompt}_{arch}) \quad (7)$$

This selection considers the temporal dependency patterns in  $X_t$ , such as choosing LSTM for strong short-term dependencies or Transformer for capturing long-range correlations. The historical performance records in  $\mathcal{K}$  guide this selection by providing evidence of each architecture's effectiveness under similar conditions.

b) *Parameter Configuration*: For each selected model  $M_i \in M_{selected}$ , the LLM determines its optimal configuration:

$$\theta_i = LLM(M_i, X_t, \mathcal{K}, \text{prompt}_{param}) \quad (8)$$

where  $\theta_i \in \Theta$  includes both architectural parameters (e.g., number of layers, hidden dimensions) and training parameters (e.g., learning rate, batch size). The configuration is based on both the current data characteristics and historical configuration effectiveness stored in  $\mathcal{K}$ .

c) *Ensemble Strategy Design*: The LLM designs an ensemble strategy  $S$  that optimally combines the selected models:

$$S = LLM(M_{selected}, \Theta, \mathcal{K}, \text{prompt}_{ensemble}) \quad (9)$$

The ensemble strategy includes both the voting mechanism and individual model weights, determined by analyzing each

model's historical reliability and current data fitness. The final ensemble model is constructed as:

$$M_{ensemble}(X_t) = \sum_{i=1}^{|M_{selected}|} w_i M_i(X_t; \theta_i) \quad (10)$$

where  $w_i$  represents the dynamic weight assigned to each model's prediction.

This knowledge-driven configuration process enables the system to adapt its prediction models dynamically based on evolving network conditions while leveraging accumulated experience from historical operations.

3) *Training Strategy*: The training strategy module optimizes the learning process of the ensemble model through LLM-driven adaptation. Given the selected training data  $\mathcal{D}_{train}$  and configured ensemble model  $M_{ensemble}$ , the training process is formulated as:

$$M_{ensemble}^* = \int_{LLM}^{train}(M_{ensemble}, \mathcal{D}_{train}, \mathcal{K}) \quad (11)$$

The training optimization process consists of three key components:

a) *Initial Parameter Configuration*: For each model  $M_i$  in the ensemble, the LLM determines optimal training parameters based on historical experience:

$$\{\eta_i, B_i\} = LLM(M_i, \mathcal{D}_{train}, \mathcal{K}, \text{prompt}_{init}) \quad (12)$$

where  $\eta_i$  is the fixed learning rate and  $B_i$  is the batch size for model  $M_i$ . These parameters remain constant throughout the training process, with their values determined by analyzing historical training patterns stored in  $\mathcal{K}$ .

b) *Loss Function Design*: The LLM constructs a composite loss function based on prediction requirements and historical error patterns:

$$\mathcal{L}(X_t, y_t) = \alpha \mathcal{L}_{ce}(X_t, y_t) + \beta \mathcal{L}_{temporal}(X_t) + \gamma \mathcal{L}_{reg}(M_{ensemble}) \quad (13)$$

where  $\mathcal{L}_{ce}$  is the cross-entropy loss for failure prediction,  $\mathcal{L}_{temporal}$  penalizes temporal inconsistency in predictions, and  $\mathcal{L}_{reg}$  provides regularization based on historical failure patterns. The weights  $\alpha, \beta, \gamma$  are determined before training:

$$[\alpha, \beta, \gamma] = LLM(\mathcal{D}_{train}, \mathcal{K}, \text{prompt}_{loss}) \quad (14)$$

c) *Performance Monitoring*: The LLM continuously evaluates prediction performance and triggers model updates when necessary:

$$\delta_t = LLM(M_{ensemble}, X_t, \mathcal{K}, \text{prompt}_{monitor}) \quad (15)$$

where  $\delta_t$  is the update decision signal. When significant performance degradation is detected, the system initiates retraining with newly configured parameters:

$$M_{ensemble}^{t+1} = \begin{cases} \text{Retrain}(M_{ensemble}, \mathcal{D}_{new}, \{\eta_i^{new}\}) & \text{if } \delta_t > \tau \\ M_{ensemble}^t & \text{otherwise} \end{cases} \quad (16)$$

This framework ensures stable training processes while maintaining the flexibility to adapt to significant changes in network conditions through model retraining with newly optimized parameters.

## B. Dual-Memory System

The dual-memory system implements a JSON-based knowledge repository that facilitates efficient experience accumulation and retrieval for LLM-driven decision making. This system addresses the context length limitations of LLMs while enabling continuous learning through structured knowledge preservation.

1) *Memory Architecture*: The short-term memory maintains a dynamic operational context for immediate decision support:

$$Mem_{short} = \{F_{current}, T_{range}, P_{model}, M_{config}, F_{recent}\} \quad (17)$$

where  $F_{current}$  represents the active feature set with selection rationale,  $T_{range}$  captures temporal context with start and end timestamps,  $P_{model}$  stores recent model performance metrics, and  $M_{config}$  maintains current model configurations and ensemble strategies.

The long-term memory implements a persistent knowledge base with activation tracking:

$$Mem_{long} = \{F_{stats}, M_{history}, E_{record}, A_{track}, F_{history}\} \quad (18)$$

where  $F_{stats}$  maintains feature statistics and selection history,  $M_{history}$  records successful model configurations,  $E_{record}$  stores historical experience entries,  $A_{track}$  tracks memory activation patterns, and  $F_{history}$  maintains valuable historical feedback:

$$F_{history} = \{(f_i, t_i, e_i) | Q(f_i) > \tau_{feedback}\} \quad (19)$$

Each feedback entry contains:

$$f_i = \{P_i, R_i, A_i\} \quad (20)$$

where  $P_i$  represents performance metrics,  $R_i$  captures LLM reasoning, and  $A_i$  records adaptation decisions.

2) *Memory Operations*: The system implements three basic memory operations:

a) *Experience Recording*: The system records new operational experiences in short-term memory:

$$Mem_{short}^{t+1} = \text{Record}(X_t, y_t, P_t, C_t) \quad (21)$$

where  $X_t$  represents current feature data,  $y_t$  is the prediction outcome,  $P_t$  contains performance metrics, and  $C_t$  includes current configurations.

b) *Memory Transfer*: The system periodically transfers valuable experiences from short-term to long-term memory:

$$Mem_{long}^{t+1} = \text{Transfer}(Mem_{short}, Mem_{long}) \quad (22)$$

This operation includes recording successful feature selections, model configurations, and performance patterns.

c) *Activation-based Cleanup*: The system implements an activation-aware cleanup mechanism:

$$A_{score}(e_i) = \lambda \frac{t_{current} - t_{last}(e_i)}{T_{max}} + (1-\lambda) \frac{n_{access}(e_i)}{N_{max}} \quad (23)$$

where  $\lambda$  balances recency and frequency of access. The cleanup operation removes entries based on their activation scores:

$$Mem_{clean} = \{e_i | A_{score}(e_i) > \tau_{active}\} \quad (24)$$

where  $\tau_{active}$  is the retention threshold.

The system maintains its effectiveness through activation-aware memory management, ensuring both efficiency and relevance in supporting LLM-driven decisions.

### C. Continuous Learning Process

The continuous learning process implements a self-evolving mechanism through LLM-driven optimization and structured feedback analysis. This process establishes a closed-loop learning cycle that continuously refines prediction capabilities based on operational experiences.

1) *Performance-Driven Feedback Generation*: The system generates structured feedback based on actual prediction results:

$$P_t = \{accuracy_t, precision_t, recall_t, stability_t\} \quad (25)$$

where performance metrics are analyzed through LLM reasoning to generate comprehensive feedback:

$$f_t = LLM(P_t, E_{record}, \text{prompt}_{analyze}) \quad (26)$$

The feedback contains component-wise assessments:

$$f_t = \{(c_i, s_i, r_i) | c_i \in \{feature, model, training\}\} \quad (27)$$

where  $s_i$  indicates performance status and  $r_i$  provides specific improvement recommendations.

2) *Actionable Improvement Strategy*: Based on the feedback analysis, the system generates concrete improvement strategies:

$$I_t = LLM(f_t, F_{history}, \text{prompt}_{improve}) \quad (28)$$

where  $I_t$  specifies actionable adjustments:

$$I_t = \{(a_i, p_i, \Delta_i) | a_i \in Actions\} \quad (29)$$

Here,  $a_i$  represents specific actions,  $p_i$  indicates their priority, and  $\Delta_i$  defines the adjustment magnitude.

3) *Self-Refinement Process*: The system implements a three-stage refinement process:

a) *Strategy Validation*: Proposed improvements are validated against historical experiences:

$$V_t = LLM(I_t, F_{history}, \text{prompt}_{validate}) \quad (30)$$

b) *Component Optimization*: Validated strategies are applied to system components:

$$C_{t+1} = Optimize(C_t, V_t, \text{prompt}_{refine}) \quad (31)$$

where  $C_t$  represents the current configuration of features, models, or training parameters.

c) *Effectiveness Assessment*: The system evaluates optimization outcomes:

$$E_t = Assess(C_{t+1}, P_{t+1}, \text{prompt}_{assess}) \quad (32)$$

The assessment results are integrated into the feedback history to guide future improvements:

$$F_{history}^{t+1} = Update(F_{history}, E_t, \text{prompt}_{update}) \quad (33)$$

This closed-loop self-refining process and its integration with the dual-memory system ensures continuous improvement while maintaining operational efficiency through experience-based optimization.

The overall framework is summarized in Algorithm 1.

## IV. EXPERIMENTAL EVALUATION

### A. Dataset Construction and Collection

1) *Infrastructure Overview*: Our experimental environment consists of a large-scale InfiniBand cluster designed for high-performance computing workloads, particularly focused on training large language models exceeding 200 billion parameters. Such training tasks demand exceptional network performance and reliability, as network failures can significantly impact model convergence and training efficiency. The cluster implements a two-layer Leaf-Spine topology with full-mesh connectivity, comprising 2,048 computing cards distributed across 8 pods. Each pod contains 256 cards connected through 8 LEAF switches, with the overall network infrastructure including 64 Leaf switches and 32 Spine switches. This architecture, compliant with NVIDIA's rail-optimized specifications, ensures optimal bandwidth utilization and minimal communication latency while maintaining network redundancy, which is crucial for sustaining the massive data transfers required in distributed LLM training.

Through our analysis, we identified two primary categories of network failures in this infrastructure: link flapping and complete link down events. These failures are particularly critical in LLM training scenarios, where even brief network interruptions can lead to significant training delays or potential loss of computation resources. The failures typically originate from optical module degradation under sustained exposure to adverse environmental conditions, particularly in scenarios involving high-temperature operation and sustained high workloads characteristic of intensive LLM training operations.

2) *Data Collection*: We developed a comprehensive data collection framework that integrates four complementary monitoring approaches. System performance counters provide detailed insights into network interface card (NIC) performance and local link status. The OpenSM subnet manager logs capture network-wide connectivity status and state transitions across all devices. Hardware diagnostics data collected through management interfaces provides information about physical components including NICs, optical modules, and cables. Additionally, network topology information is gathered to maintain a complete map of physical connections between devices.

The final processed dataset demonstrates significant scale and comprehensiveness. The performance metrics data includes approximately 77.8 billion data points collected over eight months, comprising 55 metrics per InfiniBand card (36 performance and error diagnostic metrics, 2 temperature

TABLE I  
PERFORMANCE COMPARISON OF DIFFERENT METHODS ON IB NETWORK FAILURE PREDICTION

Method	Static Scenario			Dynamic Scenario		
	P@K (%)	R@K (%)	F1@K (%)	P@K (%)	R@K (%)	F1@K (%)
<i>Individual Models</i>						
MLP	71.2±1.8	67.5±2.1	69.3±2.0	56.4±3.2	52.8±3.5	54.5±3.4
CNN	75.8±1.5	71.9±1.8	73.8±1.7	59.8±2.9	56.2±3.2	57.9±3.1
LSTM	77.2±1.3	73.4±1.6	75.2±1.5	63.5±2.6	59.9±2.9	61.6±2.8
GRU	78.1±1.2	74.2±1.5	76.1±1.4	64.8±2.5	61.2±2.8	62.9±2.7
Transformer	80.3±1.1	76.5±1.4	78.3±1.3	67.2±2.4	63.6±2.7	65.3±2.6
<i>Traditional Ensemble Methods</i>						
Majority Voting	81.5±1.0	77.8±1.2	79.6±1.1	63.8±2.2	60.2±2.5	61.9±2.4
Weighted Voting	82.4±0.9	78.6±1.1	80.4±1.0	65.9±2.1	62.3±2.4	64.0±2.3
<i>LLM-based Methods (with GPT-4o)</i>						
End-to-End Prompting	77.2±1.4	73.5±1.6	75.3±1.5	58.9±2.6	55.4±2.9	57.1±2.8
Chain-of-Thought	78.5±1.3	74.8±1.5	76.6±1.4	60.7±2.5	57.2±2.8	58.9±2.7
Self-Refine	79.1±1.2	75.4±1.4	77.2±1.3	62.3±2.4	58.8±2.7	60.5±2.6
<i>SALCA-IB with Different LLM Cores</i>						
SALCA-IB (Qwen2.5-14B)	77.8±1.3	74.1±1.5	75.9±1.4	70.2±2.2	67.1±2.5	68.6±2.4
SALCA-IB (Yi-1.5-34B)	83.2±0.9	79.5±1.1	81.3±1.0	77.5±1.8	74.2±2.1	75.8±2.0
SALCA-IB (Llama-3-70B)	84.5±0.8	80.8±1.0	82.6±0.9	79.6±1.7	76.5±2.0	78.0±1.9
<b>SALCA-IB (GPT-4o)</b>	<b>87.2±0.7</b>	<b>83.9±0.9</b>	<b>85.5±0.8</b>	<b>84.7±1.6</b>	<b>81.6±1.9</b>	<b>83.1±1.8</b>

indicators, and 17 physical parameters) collected from 256 nodes, each equipped with 8 IB cards, sampled twice per minute. Real-time state snapshots contribute an additional 40 million records, capturing every network state change. The OpenSM subnet manager logs contain 20.18 million entries documenting network events and state transitions.

For the failure prediction task, we employ a similar sampling strategy with Liu et al. [8] for training and evaluation phases. During training, we maintain a balanced 1:1 ratio between failure and normal samples to ensure the model learns effectively from both classes. For evaluation and real-world prediction scenarios, we use a more realistic 1:8 ratio that better reflects the natural distribution of failure events in production environments.

## B. Experimental Setup

1) *Implementation Details:* To investigate how LLM reasoning capabilities affect the performance of our SALCA-IB framework, we conducted experiments with four different large language models: GPT-4o (accessed via OpenAI’s API), Llama-3-70B-Instruct, Yi-1.5-34B-Chat, and Qwen2.5-14B-Instruct. Each experiment uses a single LLM as the reasoning engine throughout the entire process, allowing us to evaluate how models of different sizes and reasoning capabilities impact the framework’s effectiveness. The locally deployed models (Llama-3, Yi-1.5, and Qwen2.5) run on Nvidia H100 GPUs using vLLM for optimized inference.

The prediction model pool consists of lightweight neural networks optimized for CPU inference. These models were trained on our IB network dataset using CPU resources to ensure efficient deployment in production environments. Table III shows the configuration search space and LLM selection examples.

2) *Baseline Methods:* We designed three categories of baseline methods to evaluate the effectiveness of our SALCA-IB framework:

**Individual Deep Learning Models:** We first evaluated each model from our model pool independently. The MLP model serves as a basic deep learning baseline with its hierarchical feature extraction capability. The LSTM and GRU models represent sequence modeling approaches that capture temporal dependencies in network states. The Transformer model provides a self-attention based baseline that can model long-range dependencies. The CNN model is included to capture spatial hierarchies and local patterns in the data, which can be particularly useful for identifying localized anomalies. Each model was trained with its optimal configuration as determined by grid search.

**Traditional Ensemble Methods:** We then combined these deep learning models using conventional ensemble strategies: (1) Majority Voting, where each model contributes equally to the final prediction; (2) Weighted Voting, where weights are assigned based on each model’s validation performance; These ensemble methods represent traditional approaches to model combination without dynamic adaptation.

**LLM-based Methods:** To isolate the contribution of LLM orchestration, we implemented several LLM-based approaches using the same set of base models. These include End-to-End prompting, Chain-of-Thought prompting [18], and Self-Refine [14]. For consistency and fair comparison, each method was tested using the GPT-4o API, aligning with SALCA-IB’s LLM-driven orchestration mechanism.

## C. Evaluation Methodology

1) *Evaluation Scenarios:* The experimental evaluation, conducted on our 8-month dataset, encompasses two distinct

scenarios to comprehensively assess system performance. The static scenario evaluates models within a fixed 2-week time window, utilizing 70% of the data for training and 30% for testing, enabling assessment of baseline prediction accuracy under stable network conditions.

For dynamic scenario evaluation, we selected a continuous 16-week period from the dataset, where significant maintenance events naturally occurred. The system was initially trained on the first 2-week data segment, followed by continuous evaluation over the subsequent 14 weeks. Two major maintenance events were recorded during this period: a Week 6 maintenance involving optical module replacements and firmware updates, and a Week 12 maintenance encompassing topology adjustments and switch configuration optimization. These events created natural feature distribution shifts, allowing evaluation of the system’s adaptability to environmental changes.

2) *Evaluation Metrics*: The performance assessment employs ranking-based metrics with  $K$  set to 2% of total instances. Precision@ $K$  measures the proportion of true positives among predicted positives in top- $K$  predictions. Recall@ $K$  quantifies the ratio of detected true positives to actual positives within top- $K$  predictions. F1@ $K$  represents the harmonic mean of Precision@ $K$  and Recall@ $K$ , providing a balanced measure of prediction performance.

Statistical robustness is ensured through five independent experimental runs with different random seeds. Results are presented as mean values with standard deviations, and statistical significance is validated using paired t-tests ( $p < 0.05$ ). The system is evaluated on its ability to provide failure predictions within a 30-minute advance warning window, a critical requirement for practical deployment in production environments.

#### D. Main Results

Table I presents a comprehensive comparison of SALCA-IB against various baseline approaches. In static scenarios, SALCA-IB with GPT-4o achieves an F1@ $K$  score of  $85.5 \pm 0.8\%$ , significantly outperforming both traditional machine learning methods and existing LLM-based approaches. Specifically, it surpasses the best performing baseline (Weighted Voting:  $80.4 \pm 1.0\%$ ) by 5.1%, and demonstrates substantial improvements over individual models (Transformer:  $78.3 \pm 1.3\%$ ). The LLM-driven autonomous data selection and model optimization mechanism proves particularly effective, as evidenced by the consistent performance improvements across different model scales (14B: 75.9%, 34B: 81.3%, 70B: 82.6%, GPT-4o: 85.5%). Notably, the significant performance jump between 14B and 34B models (5.4% increase) suggests that effective data selection and model optimization require sophisticated reasoning capabilities that only larger LLMs can provide. This observation also explains why direct LLM-based prediction methods show inferior performance (Self-Refine:  $77.2 \pm 1.3\%$ ) compared to traditional approaches, validating our architectural choice of utilizing LLMs as planning cores rather than predictors.

TABLE II  
ABLATION STUDY RESULTS

Model Variant	Static F1@K (%)	Dynamic F1@K (%)
SALCA-IB (Full)	<b>85.5±0.8</b>	<b>83.1±1.8</b>
w/o LLM Planning	79.8±1.3	67.2±2.4
w/o Dual Memory	81.3±1.2	73.5±2.2
w/o Continuous Learning	82.9±1.0	76.8±2.0
Weighted Voting	80.4±1.0	64.0±2.3

The advantages of SALCA-IB become even more pronounced in dynamic scenarios where network feature distributions shift. While traditional methods experience severe performance degradation (Transformer: -13.0%, Weighted Voting: -16.4%), SALCA-IB (GPT-4o) maintains remarkably stable performance with an F1@ $K$  score of  $83.1 \pm 1.8\%$ , representing only a 2.4% decrease from its static scenario performance. This exceptional stability can be attributed to our fusion memory system, which effectively leverages both short-term memory for rapid adaptation and long-term memory for maintaining consistent performance baselines. The effectiveness of this dual-memory approach is consistently observed across different LLM scales, with even the 34B variant ( $75.8 \pm 2.0\%$ ) significantly outperforming all baseline methods.

The system’s resilience is further enhanced by our automatic evaluation feedback and closed-loop optimization mechanism, as reflected in the performance stability across different scenarios. This is evidenced by the smaller standard deviations in SALCA-IB (GPT-4o) results ( $\pm 0.8\%$  static,  $\pm 1.8\%$  dynamic) compared to traditional approaches ( $\pm 1.0$ - $2.6\%$ ). The stark contrast between SALCA-IB’s resilience and the substantial performance drops in traditional approaches (e.g., ensemble methods declining by 16-17 percentage points) demonstrates that our system successfully maintains high performance levels through continuous adaptation and optimization.

#### E. Ablation Studies

To validate the effectiveness of each key component in SALCA-IB, we conducted ablation experiments by removing individual components while keeping others intact. Table II presents the performance comparison between the full system and its variants, alongside the weighted voting baseline.

The LLM planning core demonstrates its effectiveness through the significant performance gap between the full system and the variant without LLM planning. In static scenarios, the absence of LLM planning leads to a 5.7% decrease in F1@ $K$  score, while in dynamic scenarios, the impact is even more pronounced with a 15.9% decrease. Without the LLM planning core, SALCA-IB essentially degrades into a traditional ensemble learning system with rule-based model selection and fixed data sampling strategies. The performance (79.8% in static scenarios and 67.2% in dynamic scenarios) is comparable to or slightly better than the weighted voting baseline (80.4% and 64.0%), which aligns with our expectation



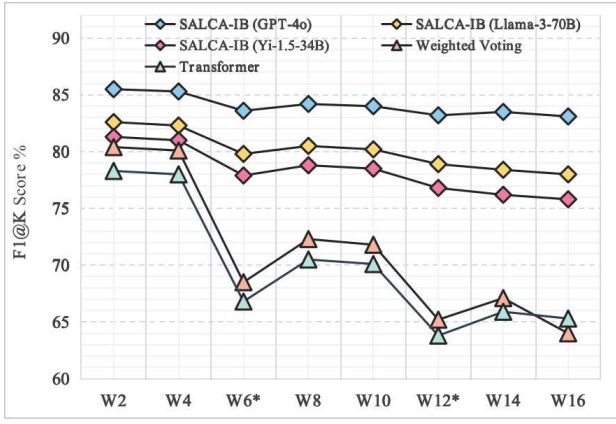


Fig. 2. Long-term performance analysis of SALCA-IB. Week 6 and Week 12 are the two maintenance events.

as both approaches rely on similar ensemble mechanisms without intelligent orchestration.

The dual memory system proves its utility in maintaining prediction accuracy, particularly under changing network conditions. When this component is removed, the system experiences a 9.6% performance degradation in dynamic scenarios. Interestingly, comparing the variants without memory (73.5%) and without continuous learning (76.8%) reveals an important insight: the absence of memory leads to a larger performance drop despite the presence of continuous learning. This suggests that the memory system provides crucial context that enables LLM to make more informed adaptations.

The continuous learning mechanism shows its value in sustaining prediction performance over time. Without this component, the system’s F1@K score decreases by 6.3% in dynamic scenarios, indicating that the feedback-driven optimization process effectively helps the system adapt to evolving network characteristics. This validates our design choice of incorporating continuous learning to enhance the system’s adaptability.

Compared to the weighted voting baseline, the full SALCA-IB system achieves superior performance in both static (85.5% vs 80.4%) and dynamic (83.1% vs 64.0%) scenarios, demonstrating the overall effectiveness of our integrated approach.

#### F. Long-term Performance Analysis

To evaluate the system’s robustness in real-world scenarios, we conducted a 16-week longitudinal study during which two major equipment maintenance events occurred (Week 6 and Week 12). As shown in Table ??, these maintenance activities significantly impacted the feature distributions and revealed striking differences in how various methods handled such environmental changes. During the first maintenance (Week 6), traditional methods experienced severe performance degradation, with Weighted Voting dropping by 11.6% (80.1% to 68.5%) and Transformer declining by 11.2% (78.0% to 66.8%). In contrast, SALCA-IB (GPT-4o) demonstrated remarkable resilience, showing only a 3.1% decrease (85.3% to

82.4%). This substantial difference in impact highlights the effectiveness of our LLM-driven planning core in adapting to feature distribution shifts.

Even more revealing is the comparison between the first and second maintenance events. During the second maintenance (Week 12), SALCA-IB (GPT-4o) showed further improved resilience with only a 1.1% performance drop (82.9% to 81.8%), significantly smaller than its first-event impact. This enhanced adaptability can be attributed to our dual-memory system, which effectively retained and leveraged the experience from the first maintenance event. The scale of LLM cores also played a crucial role in system resilience, as evidenced by the performance variations across different models - GPT-4o’s drops (3.1% and 1.1%) were notably smaller than those of Llama-3-70B (4.2% and 2.4%) and Yi-1.5-34B (4.8% and 2.9%). These results collectively demonstrate SALCA-IB’s robust performance in dynamic production environments, particularly through its effective combination of LLM-driven planning and experience-based adaptation.

#### V. CONCLUSION

This paper presents SALCA-IB, an innovative self-adaptive system for InfiniBand network failure prediction that uniquely leverages large language models as planning cores rather than direct predictors. Through extensive experiments on a production cluster with 2048 computing cards, we demonstrate that SALCA-IB significantly outperforms traditional approaches, achieving an F1@K-score of 85.5% in static scenarios and maintaining robust performance (83.1%) under dynamic network conditions. The system’s effectiveness is particularly evident during maintenance events, where it exhibits minimal performance degradation (3.1% and 1.1%) compared to traditional methods (>10%). Our work makes several key contributions to the field: demonstrating LLMs’ effectiveness as high-level planning cores for complex system optimization tasks, providing a practical dual-memory solution for knowledge accumulation in dynamic environments, and developing a continuous learning mechanism that enables sustained adaptation while maintaining prediction accuracy.

Looking forward, several promising directions emerge for future research. First, investigating the potential of more lightweight LLMs could help reduce the system’s computational overhead while maintaining performance. Second, exploring knowledge transfer mechanisms between multiple LLM agents could enhance the system’s ability to leverage cross-environment experiences through collaborative reasoning. Finally, extending the framework to support more sophisticated LLM-driven reasoning patterns and enhancing system interpretability through more detailed reasoning traces could increase its practical utility. These future directions, combined with the demonstrated success of SALCA-IB, suggest a promising path forward for developing more robust and adaptive LLM-based infrastructure management systems that can effectively support the growing demands of large-scale AI training operations.

## REFERENCES

- [1] T. Ahmed, S. Ghosh, C. Bansal, T. Zimmermann, X. Zhang, S. Rajmohan et al., "Recommending root-cause and mitigation steps for cloud incidents using large language models," in Proc. IEEE/ACM 45th Int. Conf. Software Engineering (ICSE), Melbourne, Australia, 2023, pp. 1737-1749.
- [2] K. A. Alharthi, A. Jhumka, S. Di, L. Gui, F. Cappello, S. McIntosh-Smith, "Time machine: Generative real-time model for failure (and lead time) prediction in HPC systems," in Proc. 53rd Annual IEEE/IFIP Int. Conf. Dependable Systems and Networks (DSN), 2023, pp. 508-521.
- [3] F. Antici, A. Borghesi, and Z. Kiziltan, "Online job failure prediction in an HPC system," in Euro-Par 2023: Parallel Processing Workshops, Cham: Springer, 2024, pp. 167-179.
- [4] A. Cascajo, G. Gomez-Lopez, J. Escudero-Sahuquillo, P. J. Garcia, D. E. Singh, F. Alfaro-Cortés et al., "Monitoring infiniband networks to react efficiently to congestion," IEEE Micro, vol. 43, no. 2, pp. 120-130, 2023.
- [5] A. Das, F. Mueller, C. Siegel, and A. Vishnu, "Desh: Deep learning for system health prediction of lead times to failure in HPC," in Proc. 27th Int. Symp. High-Performance Parallel and Distributed Computing, 2018, pp. 40-51.
- [6] Y. He, M. Hutton, S. Chan, R. De Gruijl, R. Govindaraju, N. Patil et al., "Understanding and mitigating hardware failures in deep learning training systems," in Proc. 50th Annual Int. Symp. Computer Architecture, 2023, pp. 1-16.
- [7] Q. Hu, Z. Ye, Z. Wang, G. Wang, M. Zhang, Q. Chen et al., "Characterization of large language model development in the datacenter," in Proc. USENIX Symp. Networked Systems Design and Implementation (NSDI), 2024, pp. 709-729.
- [8] H. Liu, Z. Li, C. Tan, R. Yang, G. Cao, Z. Liu et al., "Predicting GPU failures with high precision under deep learning workloads," in Proc. 16th ACM Int. Conf. Systems and Storage, 2023, pp. 124-135.
- [9] B. Mohammed, I. Awan, H. Ugail, and M. Younas, "Failure prediction using machine learning in a virtualised HPC system and application," Cluster Computing, vol. 22, no. 2, pp. 471-485, 2019.
- [10] B. Nie, J. Xue, S. Gupta, T. Patel, C. Engelmann, E. Smirni et al., "Machine learning models for GPU error prediction in a large scale HPC system," in Proc. 48th Annual IEEE/IFIP Int. Conf. Dependable Systems and Networks (DSN), 2018, pp. 95-106.
- [11] R. Rajachandrasekar, X. Besseron, and D. K. Panda, "Monitoring and predicting hardware failures in HPC clusters with FTB-IPMI," in Proc. IEEE 26th Int. Parallel and Distributed Processing Symp. Workshops & PhD Forum, 2012, pp. 1136-1143.
- [12] J. Su, C. Jiang, X. Jin, Y. Qiao, T. Xiao, H. Ma et al., "Large language models for forecasting and anomaly detection: A systematic literature review," arXiv preprint arXiv:2402.10350, 2024.
- [13] T. Zhang, X. Huang, W. Zhao, S. Bian, and P. Du, "LogPrompt: A log-based anomaly detection framework using prompts," in Proc. Int. Joint Conf. Neural Networks (IJCNN), 2023, pp. 1-8.
- [14] A. Madaan, N. Tandon, P. Gupta, S. Hallinan, L. Gao, S. Wiegrefe et al., "Self-Refine: Iterative refinement with self-feedback," in Advances in Neural Information Processing Systems, vol. 36, 2023, pp. 46534-46594.
- [15] Y. Weng, M. Zhu, F. Xia, B. Li, S. He, S. Liu, B. Sun, K. Liu, J. Zhao, "Large Language Models are Better Reasoners with Self-Verification," in Findings of EMNLP 2023.
- [16] G. Gladys Tyen, Hassan Mansoor, Victor Cărbune, Peter Chen, Tony Mak, "LLMs cannot find reasoning errors, but can correct them given the error location," in Findings of ACL 2024.
- [17] Kumar Shridhar, Koustuv Sinha, Andrew Cohen, Tianlu Wang, Ping Yu, Ram Pasunuru, Mrinmaya Sachan, Jason Weston, Asli Celikyilmaz, "The ART of LLM Refinement: Ask, Refine, and Trust," arXiv preprint arXiv:2311.07961, 2023.
- [18] X. Chen, S. Zhang, Y. Zhang, H. Zhang, P. Zhao, and Q. Jin, "Chain-of-Thought Prompting Elicits Reasoning in Large Language Models," in Proc. NeurIPS 2023.
- [19] Xuezhi Wang, Jason Wei, Dale Schuurmans, Quoc Le, Ed Chi, Sharan Narang, Aakanksha Chowdhery, Denny Zhou, "Self-Consistency Improves Chain of Thought Reasoning in Language Models," in Proc. ICLR 2023.
- [20] R. Krishnamurthy, A. Kumar, S. Basu, S. Maji, V. Balasubramanian, and P. Liang, "HierarchicalMem: An Adaptive Memory System for Large Language Models," in Proc. EMNLP 2023.
- [21] J. Li, Z. Yang, X. Jiang, Y. Luo, S. Zhang, and J. Yang, "Efficient Memory Management for Large Language Model Serving with Page-dAttention," in Proc. SOSP 2023.
- [22] H. Liu, K. Wang, Q. Chen, Z. Yang, J. Deng, and D. Wang, "Iterative Refinement of Large Language Model Outputs with Feedback Loops," in Proc. ACL 2023.
- [23] Z. Zhao, R. Liu, K. Chen, D. Wei, W. Shi, and D. Song, "Meta-Learning for Adaptive Large Language Models," in Proc. ICML 2023.
- [24] S. An, Z. Ma, Z. Lin, N. Zheng, J.-G. Lou, and W. Chen, "Learning from mistakes makes LLM better reasoner," arXiv preprint arXiv:2310.20689, 2024.
- [25] J. Gao, X. Ding, Y. Cui, J. Zhao, H. Wang, T. Liu, and B. Qin, "Self-evolving GPT: A lifelong autonomous experiential learner," arXiv preprint arXiv:2407.08937, 2024.
- [26] Z. Gou, Z. Shao, Y. Gong, Y. Shen, Y. Yang, N. Duan, and W. Chen, "CRITIC: Large language models can self-correct with tool-interactive critiquing," arXiv preprint arXiv:2305.11738, 2024.
- [27] S. Qiao, H. Gui, C. Lv, Q. Jia, H. Chen, and N. Zhang, "Making language models better tool learners with execution feedback," arXiv preprint arXiv:2305.13068, 2024.
- [28] N. Shinn, F. Cassano, E. Berman, A. Gopinath, K. Narasimhan, and S. Yao, "Reflexion: Language agents with verbal reinforcement learning," arXiv preprint arXiv:2303.11366, 2023.
- [29] J. Wang, J. Wang, B. Athiwaratkun, C. Zhang, and J. Zou, "Mixture-of-agents enhances large language model capabilities," arXiv preprint arXiv:2406.04692, 2024.
- [30] Z. Z. Wang, J. Mao, D. Fried, and G. Neubig, "Agent workflow memory," arXiv preprint arXiv:2409.07429, 2024.
- [31] Shunyu Yao, Jeffrey Zhao, Dian Yu, Nan Du, Izhak Shafran, Karthik Narasimhan, Yuan Cao, "ReAct: Synergizing reasoning and acting in language models," arXiv preprint arXiv:2210.03629, 2023.
- [32] D. Cao, F. Jia, S. O. Arik, T. Pfister, Y. Zheng, W. Ye, and Y. Liu, "TEMPO: Prompt-based generative pre-trained transformer for time series forecasting," arXiv preprint arXiv:2310.04948, 2024.
- [33] C. Chang, W.-Y. Wang, W.-C. Peng, and T.-F. Chen, "LLM4TS: Aligning pre-trained LLMs as data-efficient time-series forecasters," arXiv preprint arXiv:2308.08469, 2024.
- [34] N. Gruver, M. Finzi, S. Qiu, and A. G. Wilson, "Large language models are zero-shot time series forecasters," in Advances in Neural Information Processing Systems, vol. 36, 2023, pp. 19622-19635.
- [35] M. Jin, S. Wang, L. Ma, Z. Chu, J. Y. Zhang, X. Shi, P. Y. Chen, Y. Liang, Y. F. Li, S. Pan, Q. Wen, "Time-LLM: Time series forecasting by reprogramming large language models," arXiv preprint arXiv:2310.01728, 2024.
- [36] H. Xue and F. D. Salim, "PromptCast: A new prompt-based learning paradigm for time series forecasting," arXiv preprint arXiv:2210.08964, 2023.
- [37] T. Zhou, P. Niu, X. Wang, L. Sun, and R. Jin, "One fits all: Power general time series analysis by pretrained LM," in Advances in Neural Information Processing Systems, vol. 36, 2023, pp. 43322-43355.

## VI. APPENDIX

### A. The SALCA-IB Algorithm

**Algorithm 1** Self-Adaptive Learning with Continuous Assessment (SALCA-IB)

**Require:**

Network monitoring data  $\mathcal{D} = \{(X_t, y_t)\}_{t=1}^T$

Large language model  $\mathcal{L}$  with prompt templates  $\mathcal{P}$

Model pool  $\mathcal{M} = \{M_1, \dots, M_m\}$

Dual-memory system:  $Mem_{short} = \{F_{current}, T_{range}, P_{model}, M_{config}, F_{recent}\}$   
 $Mem_{long} = \{F_{stats}, M_{history}, E_{record}, A_{track}, F_{history}\}$

**Ensure:** Optimized ensemble model  $M_{ensemble}$ , Updated memory system

```

1: function INITIALIZE_SYSTEM( $\mathcal{D}, \mathcal{M}, Mem_{long}$ )
2:    $D_{train} \leftarrow LLM(\mathcal{D}, Mem_{long}, \mathcal{P}_{select})$ 
3:    $\triangleright$  Knowledge-driven data selection
4:    $(M_{selected}, \Theta, S) \leftarrow LLM(\mathcal{M}, Mem_{long}, \mathcal{P}_{config})$ 
5:    $\triangleright$  Model configuration and ensemble strategy
6:    $M_{ensemble} \leftarrow TrainEnsemble(M_{selected}, \Theta, S, D_{train})$ 
7:   return  $M_{ensemble}, D_{train}$ 
8: end function
9: function CONTINUOUSLEARNING( $M_{ensemble}, \mathcal{D}_{new}$ )
10:  while not converged do
11:     $P_t \leftarrow Predict(M_{ensemble}, X_t)$ 
12:     $\triangleright$  Generate failure predictions
13:     $E_t \leftarrow Evaluate(P_t, y_t)$ 
14:     $\triangleright$  Assess prediction performance
15:    // Feedback generation and analysis
16:     $f_t \leftarrow LLM(E_t, Mem_{long}, \mathcal{P}_{analyze})$ 
17:     $\triangleright$  Generate structured feedback
18:     $I_t \leftarrow LLM(f_t, F_{history}, \mathcal{P}_{improve})$ 
19:     $\triangleright$  Develop improvement strategies
20:     $V_t \leftarrow LLM(I_t, F_{history}, \mathcal{P}_{validate})$ 
21:     $\triangleright$  Validate proposed strategies
22:    // Memory system operations
23:     $UpdateMemory(Mem_{short}, f_t, E_t, P_t)$ 
24:     $\triangleright$  Update short-term memory
25:     $TransferMemory(Mem_{short}, Mem_{long})$ 
26:     $\triangleright$  Transfer valuable experiences
27:     $CleanupMemory(A_{track}, \tau_{active})$ 
28:     $\triangleright$  Remove inactive entries
29:    // System optimization
30:     $C_{t+1} \leftarrow Optimize(C_t, V_t, \mathcal{P}_{refine})$ 
31:     $\triangleright$  Apply validated improvements
32:     $M_{ensemble}.update(C_{t+1}, \mathcal{D}_{new})$ 
33:     $\triangleright$  Update ensemble model
34:    // Activation tracking
35:     $A_{track} \leftarrow UpdateActivation(A_{track}, f_t)$ 
36:     $\triangleright$  Update memory activation status
37:  end while
38:  return  $M_{ensemble}, Mem_{short}, Mem_{long}$ 
39: end function
40: Main process
41:  $M_{ensemble}, D_{train} \leftarrow InitializeSystem(\mathcal{D}, \mathcal{M}, Mem_{long})$ 
42:  $M_{ensemble}, Mem_{short}, Mem_{long} \leftarrow$   

     $ContinuousLearning(M_{ensemble}, \mathcal{D}_{new})$ 
43: return  $M_{ensemble}, Mem_{short}, Mem_{long}$ 

```

TABLE III  
MODEL POOL CONFIGURATION OPTIONS WITH LLM SELECTION EXAMPLES

Model Architecture Parameters	
Model Type	Parameter Range (Example Choice)
MLP	Layers: [3-6] (4) Units: [64,128,256,512] (128) Dropout: [0.1-0.5] (0.3) Width decay ratio: [1.5-3.0] (2.0)
CNN	Conv layers: [1-5] (3) Filters: [32,64,128] (64) Kernel size: [3,5,7] (3) Pooling: [Max, Average] (Max)
LSTM	Layers: [1-8] (4) Hidden units: [64,128,256,512] (128) Dropout: [0.1-0.5] (0.4) Sequence length: [10-50] (30)
GRU	Layers: [1-4] (3) Hidden units: [64,128,256,512] (256) Dropout: [0.1-0.5] (0.3) Update gate bias: [-2.0,2.0] (1.0)
Transformer	Layers: [2-8] (6) Embedding dim: [128,256,512] (256) Dropout: [0.1-0.5] (0.5) Attention heads: [4,8,16] (8)
Training Parameters	
Batch size: [32-512] (64) Learning rate: [1e-5, 1e-4, 1e-3] (5e-4) Optimizer: AdamW with weight decay [1e-5, 1e-3] (1e-4) Early stopping patience: [5-20 epochs] (10)	

TABLE IV  
APPENDIX: INFINIBAND CARD MONITORING METRICS

Category	Metric Name	Value Range
Performance & Error Diagnostics (36 metrics)	Link State	Active, Down
	Physical State	LinkUp, LinkDown
	DataPath State (x4)	DPActivated, DPDeactivated
	CDR Status (x4)	ON, OFF
	Tx/Rx CDR LOL (x4)	Binary
	Tx/Rx LOS (x4)	Binary
	Tx/Rx Fault (x4)	Binary
	FW Fault	Binary
	Error Code Response	ConfigUndefined, ...
	Eye Opening Score	[0, 100]
Temperature (2 metrics)	...	...
	Module Temperature	[-10, 80]°C
Physical Parameters (17 metrics)	Case Temperature	[-10, 85]°C
	Module Voltage	[2970, 3630]mV
	Bias Current (x4)	[0, 15]mA
	Rx Power (x4)	[-10.41, 5]dBm
	Tx Power (x4)	[-8.416, 5]dBm
	Link Speed	SDR...NDR
	Link Width	1x, 2x, 4x
	Wavelength	[840, 860]nm
	Power Class	[0, 8.0]W